Liu, Qimao

Three-level performance-based optimization method of steel frames

Published in:
Latin American Journal of Solids and Structures

DOI:
10.1590/1679-78252954

Published: 01/01/2018

Document Version
Publisher's PDF, also known as Version of record

Latin American Journal of Solids and Structures
www.lajss.org

Three-level performance-based optimization method of steel frames

Abstract
This paper describes a three-level performance-based optimization model and an estimate method of residual top displacement for steel frames at three earthquake levels. The steel frames are supposed to be elastic at frequent earthquake, inelastic and hardening at occasional and rare earthquakes, respectively. The estimate formula is derived and estimate procedure is given in detail. The estimate method only needs to use (only) one pushover analysis until steel frames yield. The yield point is obtained automatically in the proposed method. The estimate method is able to make optimization process uninterrupted. Optimal design of a 3-story 2-bay steel frame is demonstrated to validate the proposed method.

Keywords
Earthquake resistant structures, Earthquake engineering, Seismic design, Steel frames, Optimization, Optimization models.

Qimao Liu [a, b*]

[a] ABB Corporate Research Center, Vasteras, 72226, Sweden

[b] Department of Civil Engineering, Aalto University, Espoo, 02150, Finland

* qimao.liu@se.abb.com

http://dx.doi.org/10.1590/1679-78252954

Received: April 01, 2016
In Revised Form: December 15, 2017
Accepted: February 09, 2018
Available online: March 21, 2018

1 INTRODUCTION

Performance-based design refers to the methodology in which structural design criteria are expressed in terms of achieving a set of performance objectives (Ghobarah, 2001). The structural seismic design needs to be based on the defined multiple performance objectives and earthquake hazard levels. The performance objectives can be defined as three levels (i.e., serviceability, life safety, and collapse prevention) associated with three earthquake hazard levels (i.e., frequent, occasional, and rare earthquakes). The structure should has no damage at serviceability level when it meets the frequency earthquake in Eurocode 8 (European Committee for Standardization, 2004). The structure is allowed to have moderate and severe damage at life safety and collapse prevention levels when it meets occasional and rare earthquakes, respectively in Eurocode 8 (European Committee for Standardization, 2004).

Therefore, at life safety and collapse prevention levels, it is necessary to explicitly consider the inelastic behavior of the structures. The nonlinear time-history analysis is believed to be the most rigorous procedure to evaluate the inelastic behavior of structures. However, the nonlinear time-history analysis methods are believed not to be practical for everyday design because they involve computational and modeling effort, convergence problem and complexity (Liu et al., 2010; Gencturk and Elnashai, 2008). The simplified nonlinear analysis methods are preferable to evaluate the inelastic behavior of structures in civil engineering practice (Fajfar, 1999, 2000). The simplified nonlinear analysis methods are based on pushover analysis to determine structural capacity diagram and on design response spectra to represent demand diagram. The N2 method (Fajfar, 1999, 2000, 2002; Kreslin and Fajfar, 2012) and capacity spectrum method (Freeman, 1998; Zou and Chan, 2005; Gencturk and Elnashai, 2008) are typical simplified nonlinear analysis methods. The N2 method has been implemented in Eurocode 8 (European Committee for Standardization, 2004). The capacity spectrum methods have been applied in ATC 40 (Applied Technology Council, 1996) and FEMA 356 (Federal Emergency Management Agency, 2000) in different iterative procedures. The N2 method can determine performance point with no need for iteration. The simplified nonlinear analysis methods have been briefly reviewed in literature (Fajfar, 2002).

The simplified nonlinear analysis methods can obtain seismic demands (top displacement, inter-story drifts, etc.) at different hazard levels. The seismic demands are compared with performance targets (specified limits on top displacement, inter-story drifts etc.) for the relevant performance levels. If the seismic demands are equal to or less than performance targets, it means the structures perform well at different hazard levels. If the seismic demands are greater than performance targets, the structural performance is unsatisfied at different hazard levels. The new structures must be modified and the existing structures must be strengthened until the structures perform well at different hazard levels. Therefore, it is still tedious to design a new structure which can perform well at

different hazard levels using the simplified nonlinear analysis methods, although it may be relatively simple to evaluate performance of the existing structures at different hazard levels.

The author ever proposed an optimization procedure for seismic design of steel frames for multi-performance and multi-hazard levels (Liu and Paavola 2015). However, the inter-story drifts are directly treated in the constraints, for a building with many stories, it is not convenient to implement. In this paper, a novel method to estimate residual top displacements of steel frames at different hazard levels is developed. A three-level performance-based optimization model is proposed. The paper is arranged as follows. In section 2, three performance levels and associated three hazard levels are defined. In section 3, elastic and inelastic demand spectra in AD format are obtained based on elastic acceleration response spectrum in EC8. In section 4, a proposed method to obtain capacity spectrum diagram is developed based on the N2 method. Compared with the N2 method, the proposed method use (only) one pushover analysis until steel frames yield. It also doesn't need any engineering judgements to get the yield point. In section 5, reduction factor and ductility factor are determined. In section 6, an estimate method of residual top displacement is developed for three-level performance-based design. In section 7, computational procedure of residual top displacement is given in detail. In section 8, a three-level performance-based optimization model is formulated based on the residual top displacements. Finally, as the illustration of the developed approach, optimal design of a 3-story 2-bay steel frame is demonstrated using ANSYS software.

2 DEFINITION OF PERFORMANCE AND HAZARD LEVELS

The performance targets are specified limits on any response parameters, i.e., top displacement, inter-story drifts, stresses, strains, etc., at relevant performance levels. The performance objectives require that the structural seismic demands are equal to or less than performance targets at relevant performance levels. The top displacement of the MDOF system is a good indicator of the global deformation of the buildings subjected to earthquake loading. The top displacement is often taken as the global seismic demand in performance based design (Kreslin and Fajfar, 2012; Fajfar, 1999, 2000, 2002; Ghobarah, 2001; Zou and Chan, 2005; Gencturk and Elnashai, 2008). However, the top displacement can not reveal the global damage degree of the buildings subjected to severe ground motions. The residual top displacement is not only a good indicator of the global deformation of the buildings subjected to earthquake loading, but also can reveal the global damage degree of the buildings subjected to severe ground motions. In multi-level performance based design, the residual deformation of the buildings is present at the life safety and collapse prevention levels. In this paper, the seismic demand of steel frame is the residual top displacement. The limits on residual top displacement are performance targets. The performance objectives require that the residual top displacement of steel frame is equal to or less than the limits on residual top displacement at relevant performance levels. The three performance levels, corresponding damage states and limits on residual top displacement are defined in Table 1. The performance levels are associated with earthquake hazard and design levels. Three earthquake hazard levels associated with the three performance levels are proposed in Table 2.

3 SEISMIC DEMAND DIAGRAM

According to the preceding definition, the seismic demand diagram is the elastic acceleration response spectrum at serviceability level, and inelastic acceleration response spectra at life-safety protection and collapse prevention levels.

Table 1: *Three performance levels, corresponding damage states and limits on residual displacement.*

Performance levels	Damage states	Limits on residual top displacement
Serviceability	No damage	$\left[D_{tp}^{(1)} \right] = 0$
Life safety	Moderate damage and repairable	$\left[D_{tp}^{(2)} \right] = 5$ cm
Collapse prevention	Severe damage	$\left[D_{tp}^{(3)} \right] = 15$ cm

Table 2: *Proposed earthquake hazard levels.*

Earthquake frequency	Return period for years	Probability of exceedance	Peak ground accelerations (in this paper)
Frequent	43	50% in 30 years	$a_g^{(1)}$ (0.15g)
Occasional	72	50% in 50 years	$a_g^{(2)}$ (0.40g)
Rare	475	10% in 50 years	$a_g^{(3)}$ (0.60g)

3.1 Horizontal elastic acceleration response spectrum in AD format

The elastic response acceleration spectrum $S_{ae}(T)$ for the horizontal components of seismic action is defined in Eurocode 8 (European Committee for Standardization, 2004) as

$$\begin{aligned}
&0 \le T \le T_B: \quad S_{ae}(T) = a_g S\left[1+\frac{T}{T_B}(2.5\eta-1)\right] \\
&T_B \le T \le T_C: \quad S_{ae}(T) = 2.5 a_g S \eta \\
&T_C \le T \le T_D: \quad S_{ae}(T) = 2.5 a_g S \eta \frac{T_C}{T} \\
&T_D \le T \le 4s: \quad S_{ae}(T) = 2.5 a_g S \eta \frac{T_C T_D}{T^2}
\end{aligned} \tag{1}$$

where $S_{ae}(T)$ is the elastic response spectrum; T is the vibration period of a linear single-degree-of-freedom system; a_g is the design ground acceleration on type A ground; T_B is the lower limit of the period of the constant spectral acceleration branch; T_C is the upper limit of the period of the constant spectral acceleration branch; T_D is the value defining the beginning of the constant displacement response range of the spectrum; S is the soil factor and η is the damping correction factor with a reference value of $\eta = 1$ for 5% viscous damping ratio. For ground type A, $S = 1.0$, $T_B = 0.15$ s, $T_C = 0.4$ s, $T_D = 2.0$ s.

For an elastic SDOF system, the displacement response spectrum is

$$S_{de}(T) = \frac{T^2}{4\pi^2} S_{ae}(T) \tag{2}$$

where $S_{de}(T)$ is the value in the displacement spectrum corresponding to the period T and a fixed viscous damping ratio.

Elastic response spectrum in AD format is obtained by Eqs. (1) and (2). For the horizontal elastic acceleration response spectrum defined in EC8, the cut-off period is obviously 2 s in AD format.

3.2 Horizontal inelastic acceleration response spectrum in AD format

The relationship between inelastic response spectrum and elastic response spectrum (Vidic et al., 1994) is

$$S_a(T) = \frac{S_{ae}(T)}{R_\mu} \tag{3}$$

$$S_d(T) = \frac{\mu}{R_\mu} S_{de}(T) \tag{4}$$

where $S_d(T)$ and $S_a(T)$ are the values in the displacement and acceleration spectra, respectively, corresponding to the period T and a fixed viscous damping ratio (5%). R_μ is the reduction factor and μ is ductility factor.

By substituting Eqs. (3) and (4) into Eq. (2), we obtain the inelastic response spectrum function in AD format,

$$S_d(T) = \mu \frac{T^2}{4\pi^2} S_a(T) \tag{5}$$

For a bilinear spectrum,

$$R_\mu = (\mu-1)\frac{T}{T_C} + 1 \quad T < T_C \tag{6}$$

$$R_\mu = \mu \quad T \geq T_C \tag{7}$$

The reduction factor R_μ and the ductility factor μ are related to both the structural response and the elastic acceleration response spectrum.

4 STRUCTURAL CAPACITY DIAGRAM

4.1 Base shear-Top displacement diagram (MDOF system)

The nonlinear static analysis (also called pushover analysis) is used to obtain the base shear force (V)-top displacement (D_t) diagram for MDOF system. A monotonically increasing pattern of lateral forces is applied to structures in pushover analysis. A planar steel frame shown in Figure 1 is assumed where n is the number of the story, the height of the i th story is h_i and the mass of the i th story is m_i. The inverted triangular load pattern with maximum loading at top and zero loading at the ground level is employed in this paper. It is assumed that the lateral force at the i th story shown in Figure 1 is proportional to the component of the assumed displacement shape Φ_i weighted by the story mass m_i (Fajfar and Gaspersic, 1996),

$$P_i = p m_i \Phi_i \tag{8}$$

where the component of the assumed displacement shape Φ_i is

$$\Phi_i = \frac{\sum_{k=1}^{i} h_k}{\sum_{k=1}^{n} h_k} \tag{9}$$

where p controls the magnitude of the lateral loads of steel frames. The displacement shape follows the first vibration mode of the building.

Therefore, the base shear force V is

$$V = \sum_{i=1}^{n} P_i = p \sum_{i=1}^{n} m_i \Phi_i = p m^* \tag{10}$$

where $m^* = \sum_{i=1}^{n} m_i \Phi_i$ is the equivalent mass of the SDOF system.

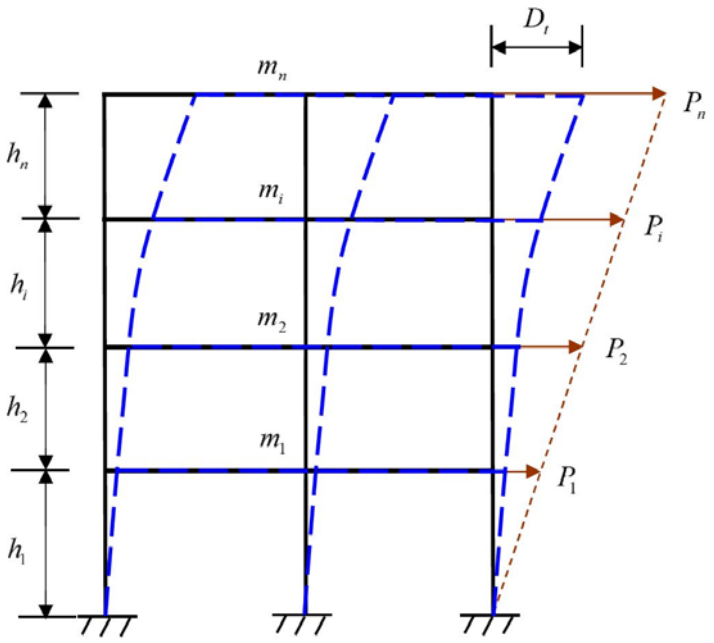

Figure 1: *n-story steel frame.*

The equal loading steps are applied to steel frame in pushover analysis. The loading step size ΔP_i at the i th story is

$$\Delta P_i = \frac{p}{c} m_i \Phi_i = \Delta p m_i \Phi_i \tag{11}$$

where $\Delta p = \frac{p}{c}$, and c is a constant integer.

The increment of base shear force is

$$\Delta V = \sum_{i=1}^{n} \Delta P_i \tag{12}$$

In the base shear force (V)-top displacement (D_t) diagram shown in Figure 2, ΔV_j and ΔD_{tj} are the increment of base shear force and increment of top displacement at the j th load step, respectively.

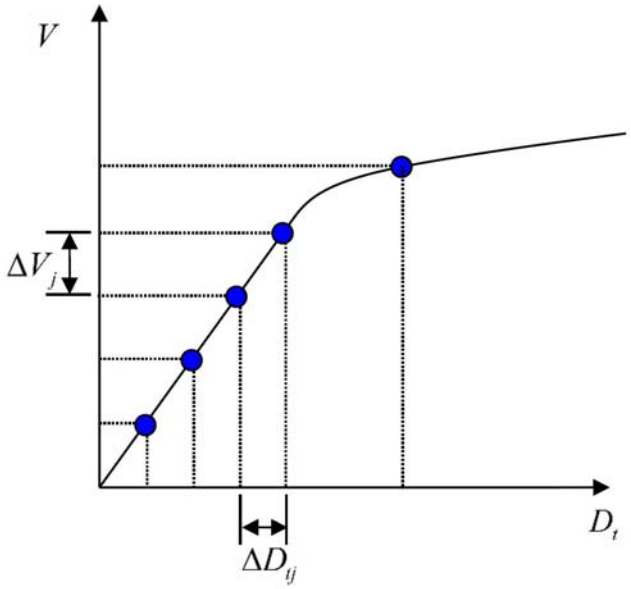

Figure 2: V *-*D_t *diagram.*

4.2 The F^* - D^* diagram, yield point and elastic period (equivalent SDOF system)

The displacement of the equivalent SDOF system is

$$D^* = \frac{D_t}{\Gamma} \tag{13}$$

The base shear force of the equivalent SDOF system is

$$F^* = \frac{V}{\Gamma} \tag{14}$$

where Γ is a constant and calculated as

$$\Gamma = \frac{\sum_{i=1}^{n} m_i \Phi_i}{\sum_{i=1}^{n} m_i \Phi_i^2} = \frac{m^*}{\sum_{i=1}^{n} m_i \Phi_i^2} \tag{15}$$

Provided that both shear force (V) and top displacement (D_t) are divided by Γ, the force - displacement relationship determined for the MDOF system, i.e., V - D_t diagram, becomes the shear force and displacement relationship for the equivalent SDOF system, i.e., the shear force F^* and displacement D^* diagram shown in Figure 3.

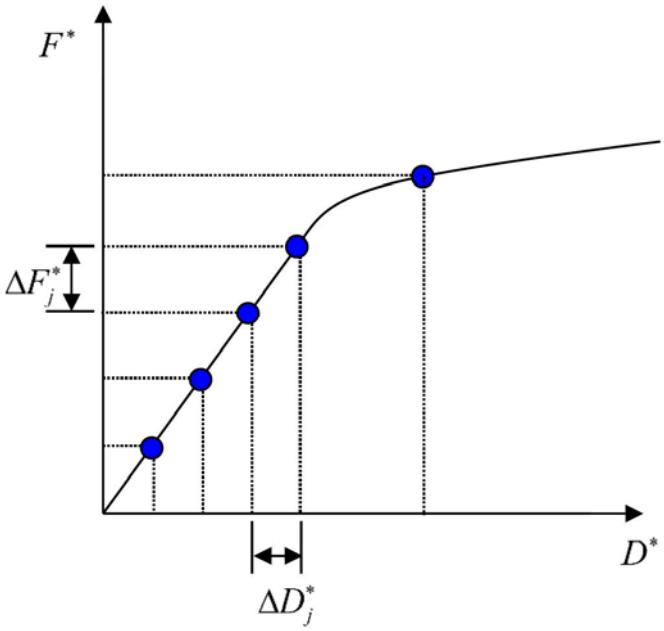

Figure 3: *F^* - D^* diagram.*

In Figure 3, ΔF_j^* and ΔD_j^* are shear force increment and displacement increment of the equivalent SDOF system at the jth load step, respectively.

$$\Delta F_j^* = \frac{\Delta V_j}{\Gamma} \tag{16}$$

$$\Delta D_j^* = \frac{\Delta D_{tj}}{\Gamma} \tag{17}$$

In this paper, the steel frame is assumed to yield if the following inequalities are true at the y th load step,

$$\frac{\Delta F_1^*}{\Delta D_1^*} \geq \gamma \frac{\Delta F_y^*}{\Delta D_y^*} \tag{18}$$

OR

$$\Delta D_y^* \geq \gamma \Delta D_1^* \tag{19}$$

where γ is a constant and greater than 1. For structure steel, the modulus of elasticity is much greater than the tangent modulus, in this paper, $\gamma = 2$ or bigger can be enough to judge that the yielding happens.

Therefore, the displacement at the yield point in F^* - D^* diagram is

$$D_y^* = \sum_{k=1}^{y} \Delta D_k^* \tag{20}$$

The shear force at the yield point in F^* - D^* diagram is

$$F_y^* = \sum_{k=1}^{y} \Delta F_k^* \tag{21}$$

In this paper, the post-yield stiffness is idealized to be zero (Aschheim and Black 2000). The idealized F^* - D^* diagram is shown in Figure 4. The elastic period of the idealized bilinear system can be calculated as

$$T^* = 2\pi \sqrt{\frac{m^* D_y^*}{F_y^*}} \tag{22}$$

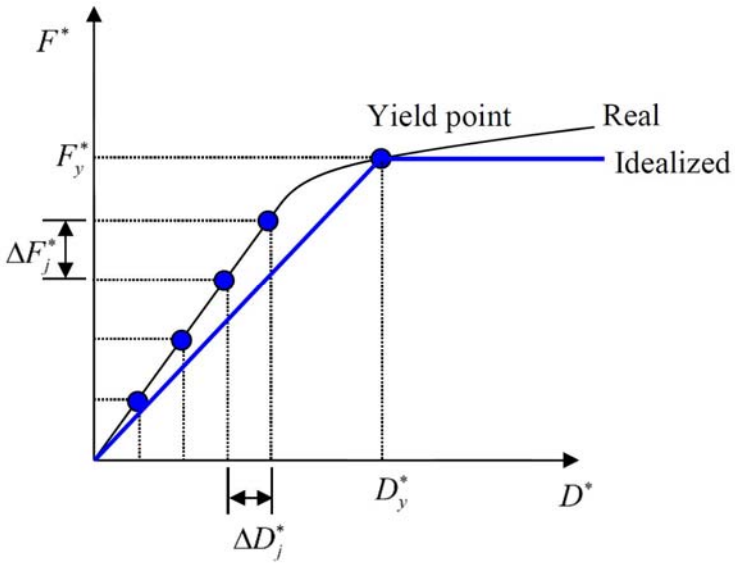

Figure 4: *Idealized F^* - D^* diagram (thick line).*

4.3 Capacity diagram in AD format

The capacity diagram in AD format shown in Figure 5 is obtained by dividing the forces in the force-deformation diagram, i.e., the idealized F^* - D^* diagram, by the equivalent mass m^*.

$$S_a = \frac{F^*}{m^*} \tag{23}$$

In this paper, the pushover analysis is used until the steel frames yield and the capacity diagram is obtained. It is relatively easier to succeed in performing pushover analysis until a steel frame yields than until the frame collapses. It doesn't need any engineering judgements to get the yield point. Therefore, it can make the optimization process uninterrupted.

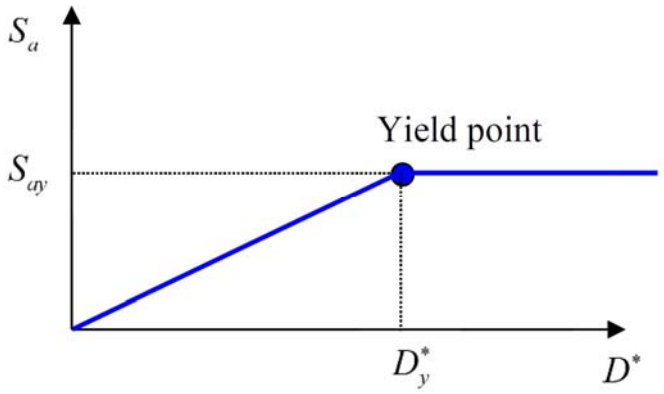

Figure 5: *Capacity diagram in AD format.*

5 DETERMINATION OF REDUCTION FACTOR AND DUCTILITY FACTOR

Elastic response spectrum in AD format, inelastic spectrum in AD format and capacity diagram in AD format are plotted in the same picture shown in Figure 6 ($T^* \geq T_C$) or Figure 7 ($T^* < T_C$). The reduction factor R_u is defined as the ratio between the accelerations corresponding to the elastic and inelastic systems,

$$R_u = \frac{S_{ae}(T^*)}{S_{ay}} \tag{24}$$

where $S_{ae}(T^*)$ is the acceleration value of the elastic spectrum diagram at the period T^* and S_{ay} is the yield acceleration shown in Figure 6 or Figure 7.

If $S_{ay} \geq S_{ae}(T^*)$, i.e., $R_u \leq 1$, the steel frame response is elastic. Therefore, the ductility factor μ is

$$\mu = 1 \text{ when } R_u \leq 1 \tag{25}$$

If $S_{ay} < S_{ae}(T^*)$, i.e., $R_u > 1$, the steel frame response is inelastic. The ductility factor μ can be calculated as follows:

If $T^* \geq T_C$ (shown in Figure 6),

$$\mu = \frac{S_d}{D_y^*} = \frac{S_{de}(T^*)}{D_y^*} = \frac{S_{ae}(T^*)}{S_{ay}} = R_u \tag{26}$$

where $S_{de}(T^*)$ is the displacement value of the elastic spectrum at the period T^* and S_d is displacement value at the intersection of the inelastic spectrum diagram and capacity diagram shown in Figure 6 and Figure 7.

If $T^* < T_C$ (shown in Figure 7),

$$\mu = \left(R_\mu - 1\right)\frac{T_C}{T^*} + 1 \tag{27}$$

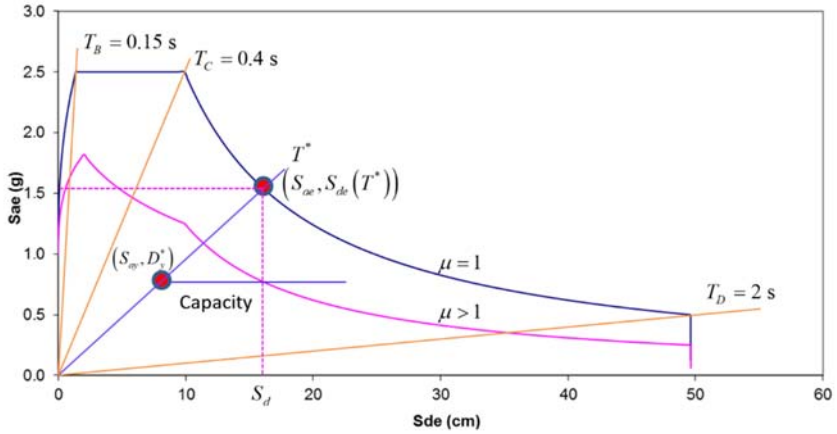

Figure 6: *Elastic spectrum AD format, inelastic spectrum AD format and capacity diagram ($T^* \geq T_C$).*

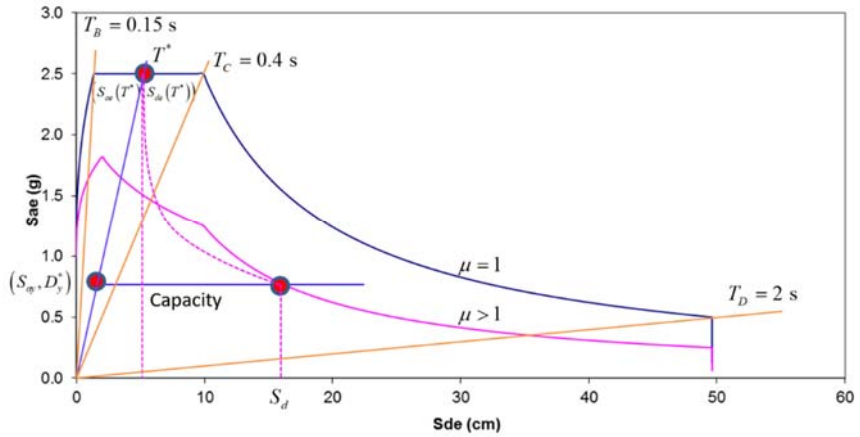

Figure 7: *Elastic spectrum AD format, inelastic spectrum AD format and capacity diagram ($T^* < T_C$).*

6 ESTIMATE OF RESIDUAL DEFORMATION

For the case of three performance levels (i.e., serviceability, life safety, and collapse prevention), the three corresponding structural characteristics (i.e., stiffness, strength and deformation capacity) dominate the performances as shown in Figure 8. The typical performance curve of the steel frames shown in Figure 8 indicates that no residual top displacement is present at serviceability level, moderate and tolerable residual top displacement is present at life-safety level, and large residual top displacement is present at collapse prevention level. Although the permanent deformation exists at life safety and collapse prevention levels, the steel frame is in strong hardening phase at serviceability and in weak hardening phase at collapse prevention, respectively.

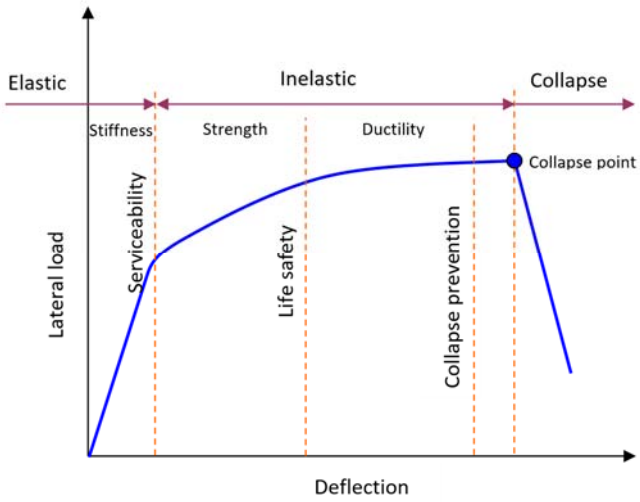

Figure 8: *Typical performance curve of steel frames.*

The displacement demand of the equivalent SDOF system can be determined from the definition of ductility as

$$S_d = \mu D_y^* \tag{28}$$

The displacement demand of the equivalent SDOF system is transformed back to the top displacement of the MDOF system,

$$D_t = \Gamma S_d = \Gamma \mu D_y^* \tag{29}$$

If the steel frame is at elastic phase (the ductility factor $\mu = 1$), No residual top displacement is present after earthquake, i.e., $D_{tp} = 0$.

If the steel frame is at inelastic and hardening phase (the ductility factor $\mu > 1$) as shown in Figure 9, according to the idealized F^*-D^* diagram, the residual displacement demand of the equivalent SDOF system can be estimated as

$$D_p^* = \mu D_y^* - D_e^* = \mu D_y^* - \frac{\Delta D_1^*}{\Delta F_1^*} F_y^* \tag{30}$$

where D_e^* is the elastic displacement.

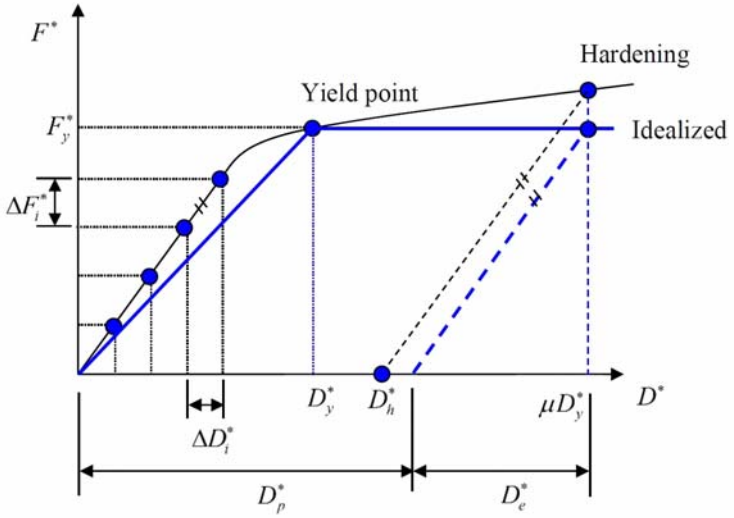

Figure 9: *Real and idealized F^*-D^* diagram.*

If the steel frame is still at hardening phase as shown in Figure 9, the estimated value of the residual top displacement of the steel frame D_p^* is greater than the real residual top displacement D_h^*. Therefore, the estimated value of the residual top displacement is conservative in Eq. (30).

The residual displacement of the equivalent SDOF system is transformed back to the top residual displacement of the MDOF system,

$$D_{tp} = \Gamma D_p^* = \Gamma\left(\mu D_y^* - \frac{\Delta D_1^*}{\Delta F_1^*} F_y^*\right) \tag{31}$$

As shown in Figure 8, the steel frame is in elastic phase at serviceability, in strong hardening phase and in weak hardening phase at life safety and collapse prevention levels, respectively. Therefore, the residual top displacement of steel frame at serviceability, life safety and collapse prevention levels, can be estimated as: if $\mu = 1$, $D_{tp} = 0$, if $\mu > 1$, the residual top displacement is calculated by using Eq. (31).

7 COMPUTATIONAL PROCEDURE FOR RESIDUAL TOP DISPLACEMENT

The Eq. (31) is used to estimate the residual top displacement of the MDOF system when the steel frame response is at elastic phase or inelastic and hardening phase. The detail of computational procedure is:

Step 1 Perform pushover analysis with the equal loading step size controlled by Eq. (11) until the steel frame yields (Inequalities Eq. (18) or Eq. (19) is true).

Step 2 Obtain the yield point $\left(D_y^*, F_y^*\right)$ using Eq. (20) and Eq. (21).

Step 3 Calculate the elastic period T^* of the equivalent SDOF system using Eq. (22).

Step 4 Calculate the reduction factor R_u with Eq. (24).

Step 5 If $R_u \le 1$, then $\mu = 1$, the residual top displacement is $D_{tp} = 0$. If $R_u > 1$, calculate the reduction factor μ with Eq. (26) (if $T^* \ge T_C$) or Eq. (27) (if $T^* < T_C$). Estimate the residual top displacement D_{tp} using Eq. (31).

8 THREE-LEVEL PERFORMANCE OPTIMIZATION MODEL

The type A ground motion is defined with the elastic acceleration response spectrum according to Eq. (1), which has been normalized to peak ground acceleration a_g equal to $a_g^{(1)}$, $a_g^{(2)}$ and $a_g^{(3)}$ at frequent, occasional and rare earthquake, respectively. The design ground accelerations for the three level performances depend on different design codes and can be chosen by structural engineers. The residual top displacements of steel frames can be estimated by the computational procedure in section 7. The residual top displacements are denoted as $D_{tp}^{(1)}$, $D_{tp}^{(2)}$ and $D_{tp}^{(3)}$ at frequent, occasional and rare earthquake, respectively. $\left[D_{tp}^{(1)}\right]$, $\left[D_{tp}^{(2)}\right]$ and $\left[D_{tp}^{(3)}\right]$ are the limits on residual top displacements related to serviceability, life safety and collapse prevention levels, respectively.

The three-level performance optimization model is proposed as

$$\begin{aligned}
&\text{Find } \boldsymbol{d}\\
&\text{Min } M(\boldsymbol{d})\\
&S.T.\ D_{tp}^{(1)}(\boldsymbol{d}) \le \left[D_{tp}^{(1)}\right]\\
&\quad D_{tp}^{(2)}(\boldsymbol{d}) \le \left[D_{tp}^{(2)}\right]\\
&\quad D_{tp}^{(3)}(\boldsymbol{d}) \le \left[D_{tp}^{(3)}\right]\\
&\quad \underline{d}_i \le d_i \le \overline{d}_i \quad (i = 1, 2, \cdots, N)
\end{aligned} \tag{32}$$

where $\boldsymbol{d}$ and $M\left(\boldsymbol{d}\right)$ are the vector of design variables and mass of steel frame, respectively. d_i, $\underline{d}_i$, and $\overline{d}_i$ are the ith design variable, its lower and upper boundary, respectively. N is the number of design variables. The residual top displacements ($D_{tp}^{(1)}$, $D_{tp}^{(2)}$, and $D_{tp}^{(3)}$) are dependent on the vector of design variables $\boldsymbol{d}$.

In this paper, the first-order optimization method of ANSYS is employed to solve the optimization model of Eq. (32). In the first-order optimization method, the sensitivity analysis technique is used to construct optimization algorithm and determine the searching direction. ANSY uses the finite-difference methods to perform sensitivity analysis. The first-order method converts the constrained optimization problem into a series of unconstrained optimization problems by using penalty function methods. According to the lateral load pattern of Eq. (8), the relation between the residual top displacements $D_{tp}^{j}\ \left(j=1,2,3\right)$ and residual inter-story drifts $dr_i\ \left(i=1,2,\cdots,n\right)$ is

$$D_{tp}^{j}=\sum_{i=1}^{n}dr_i \tag{33}$$

Assumed that the kth story of the structure is weak/soft story, the residual inter-story drift of the kth story is the dominant component in the contribution to the residual top displacement.

$$D_{tp}^{j}\approx dr_k \tag{34}$$

The design variable of columns at the kth story is d_k. Differentiating Eq. (34) with respect to design variable d_k, we have

$$\frac{\partial D_{tp}^{j}}{\partial d_k}\approx\frac{\partial dr_k}{\partial d_k} \tag{35}$$

Since the kth story of the structure is weak/soft story, the first order sensitivity $\frac{\partial dr_k}{\partial d_k}$ will be very large. In Eq. (35), the first order sensitivity of residual top displacement, i.e., $\frac{\partial D_{tp}^{j}}{\partial d_k}$, will become very large. The design with weak/soft story is impossible to be chosen as the optimum design.

Therefore, although there are no explicit constraints on inter-story drifts in three-level performance optimization model of Eq. (32), the inter-story drifts (local seismic demand) are indirectly constrained by using residual top displacement constraints, lateral load pattern (inverted triangle) and sensitivity analysis technique.

9 EXAMPLE

9.1 Optimal design of a 3-story 2-bay steel frame

A three-story two-bay steel frame shown in Figure 10 is fixed at the ground. The height of the first, second and third stories are $h_1=5.4m$, $h_2=3.6m$ and $h_3=3.6m$, respectively. The steel frame consists of 4 groups including B1, C1, C2, and C3 shown in Figure 10. All the members are H-shape section shown in Figure 10. The design variables are the size of flanges and webs also shown in Figure 10. The design variable vector is

$$\boldsymbol{d}=\left[h_{bf},t_{bf},h_{bw},t_{bw},h_{1cf},t_{1cf},h_{1cw},t_{1cw},h_{2cf},t_{2cf},h_{2cw},t_{2cw},h_{3cf},t_{3cf},h_{3cw},t_{3cw}\right]$$

The Beam189 element is used to analyze the steel frame. Beam189 is a 3-D 3-node element. This element is well-suited for linear, large rotation, and large strain nonlinear analysis. The Beam element is developed by Simo and Vu-Quoc (1986), and Ibrahimbegovic (1995). The pushover analysis is carried out using ANSYS software. The properties of material are defined as: Modulus of elasticity $E=200\ \mathrm{GPa}$, Poisson's ratio $\nu=0.3$, Yield stress $\sigma_y=235\ \mathrm{MPa}$ and Secant modulus of plasticity $E_s=1.035\ \mathrm{MPa}$, Density $\rho=7857\ \mathrm{kg/m^3}$. The mass of every floor is assumed to be 1000 kg. The design space, i.e., lower and upper limits, is shown in Table 3.

Table 3: *Design space, initial and optimum designs.*

		Initial design	Optimum design	Design space	
				Lower limits	Upper limits
Beam **B1** (mm)	Flange width	150	130	100	180
	Flange thickness	17	12	8	22
	Web depth	400	319	205	600
	Web thickness	14	7	6	20
Column **C1** (mm)	Flange width	150	147	100	180
	Flange thickness	17	16	5	22
	Web depth	400	431	250	600
	Web thickness	14	11	4	20
Column **C2** (mm)	Flange width	150	143	100	180
	Flange thickness	17	14	5	22
	Web depth	400	355	250	600
	Web thickness	14	11	4	20
Column **C3** (mm)	Flange width	150	143	100	180
	Flange thickness	17	14	5	22
	Web depth	400	349	250	600
	Web thickness	14	11	4	20
Structural mass (kg)		6218	4014		
Period of SDOF, T^*, (s)		0.164	0.216		
Yield displacement of SDOF, D_y^*, (cm)		9.13	11.10		
Ductility factor, μ	1st level	1.000	1.000		
	2nd level	1.000	1.039		
	3rd level	1.176	1.985		
Top displacement, D_t, (cm)	1st level	3.10	4.42		
	2nd level	8.25	14.59	Note: $D_t = \Gamma \mu D_y^*$	
	3rd level	13.57	27.88		

In this example, the peak ground accelerations are assumed as $a_g^{(1)} = 0.15$ g, $a_g^{(2)} = 0.4$ g and $a_g^{(3)} = 0.6$ g at frequent, occasional and rare earthquake, respectively. The limits on residual top displacements are assumed as $\left[D_{tp}^{(1)} \right] = 0$, $\left[D_{tp}^{(2)} \right] = 5$ cm, and $\left[D_{tp}^{(3)} \right] = 15$ cm.

The first-order optimization method of ANSYS is employed to solve the optimization model of Eq. (32). The first-order method will perform a maximum of 30 iterations upon execution, using a line search step equal to 100% of the maximum possible value, and a 0.200% difference applied to the design variables to obtain the first-order sensitivity. The tolerance of the objective function is 10 kg, i.e., the algorithm converges if the difference between the two adjacent objective values, achieved by the adjacent two linear searching, is less than 10 kg. Starting with the initial design shown in Table 3, the first-order optimization method converges at the sixth iteration to obtain the optimum design shown in Table 3. In the optimization process, the frame mass, ductility factor, and residual top displacements at the serviceability, life safety and collapse prevention levels are shown in Figures 11, 12, and 13, respectively.

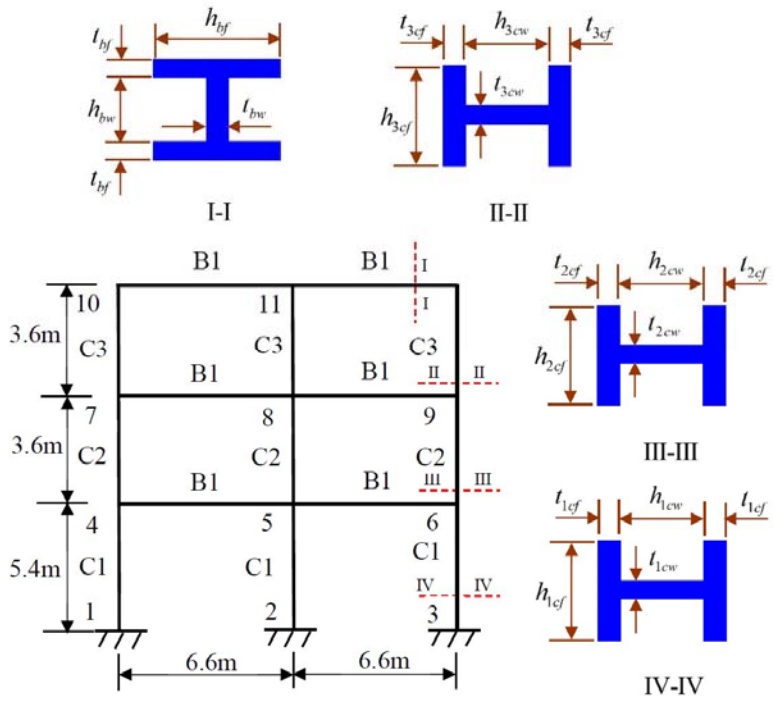

Figure 10: *Three-story steel frame with H-shape sections of members.*

9.2 Observation of optimum design

Table 3 shows that the residual top displacement of the optimum design at collapse prevention level is 14.68 cm and the upper limit of the design space is 15 cm, and the residual top displacement of the optimum design at life safety level is 1.40 cm and the upper limit of the design space is 5 cm. Therefore, the constraint of the residual top displacement is active at collapse prevention level, not active at life safety level. If the constraint upper limit of residual top displacement at collapse prevention level in this mathematical model is changed, the different optimum design will be achieved. The optimum design is compared with the initial design shown in Table 3, and in Figures 11, 12 and 13. The mass of optimum design decreases. The period and yield displacement of the equivalent SDOF increase, the ductility factor increases, and the top displacements of the steel frame at serviceability, life safety, and collapse prevention levels increase.

Table 4: *Inter-story drifts of optimum design (units: cm).*

	1st-story	2nd-story	3rd-story
Serviceability level	1.79	1.56	1.07
Life safety level	6.18	5.08	3.33
Collapse prevention level	13.53	9.14	5.25

Table 5: *Inter-story drift ratio of optimum design.*

	1st-story	2nd-story	3rd-story
Serviceability level	0.003	0.004	0.003
Life safety level	0.011	0.014	0.009
Collapse prevention level	0.025	0.025	0.015

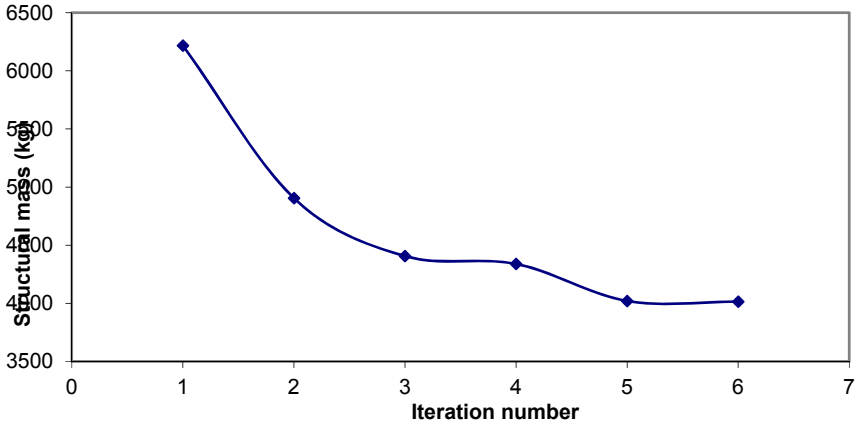

Figure 11: *Objective function variation in optimization process.*

In the design codes, the inter-story drifts must be verified to satisfy the limitations. Therefore, the pushover analyses of the optimum design should be used once again. According to the top displacements shown in Table 3, the pushover analysis stops if the top displacement is equal or greater than 27.88 cm at collapse prevention level, equal or greater than 14.59 cm at life safety level, equal or greater than 4.42 cm at serviceability level. The results show that the pushover analysis stops at 27.92 cm, 14.595 cm, and 4.424 cm, at collapse prevention, life safety, and serviceability levels, respectively. The inter-story drifts of the optimum design at collapse prevention, life safety, and serviceability levels are listed in Table 4. The pushover analysis process at collapse prevention level is shown in Figure 14. The diagrams of top displacement, inter-story drifts shown in Figure 14 indicate that the steel frame is at the hardening phase at collapse prevention level. Therefore, the estimated method of the residual top displacement proposed in this paper is reasonable. The inter-story drift and top displacement diagrams of the optimum design at serviceability, life safety, and collapse prevention levels are shown in Figure 15. The inter-story drift ratios of the optimum design in Table 5 indicate that the distribution of inter-story drift ratios are relatively uniform at serviceability, life safety, and collapse prevention levels, respectively.

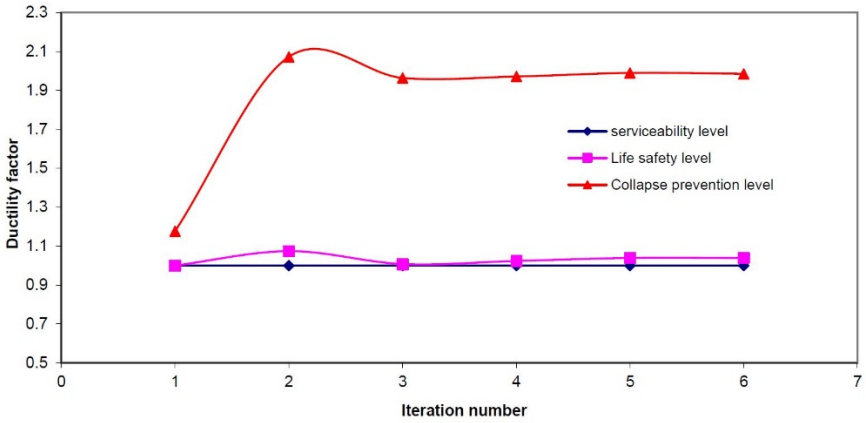

Figure 12: *Ductility factor variation in optimization process.*

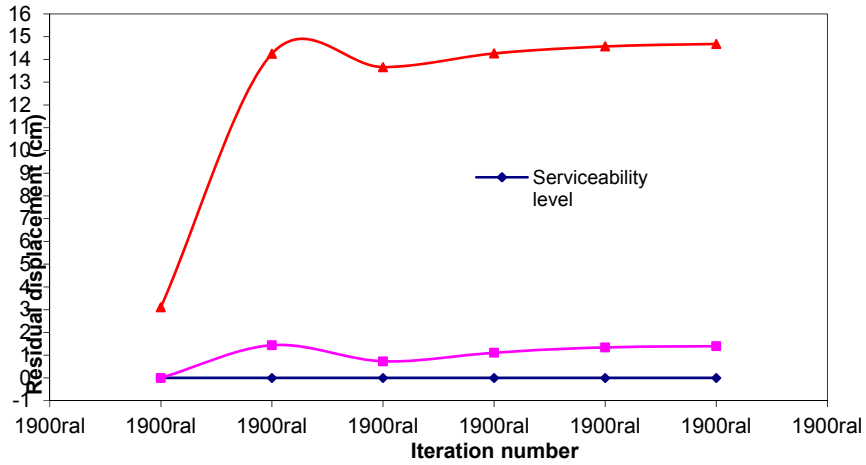

Figure 13: *Residual top displacement variation in optimization process.*

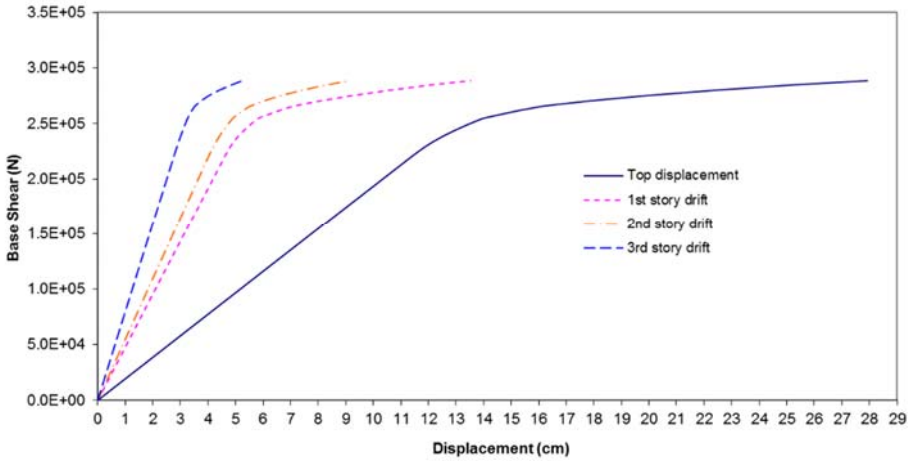

Figure 14: *Pushover analysis to top displacement 27.92 cm (≥27.88 cm) for optimum design.*

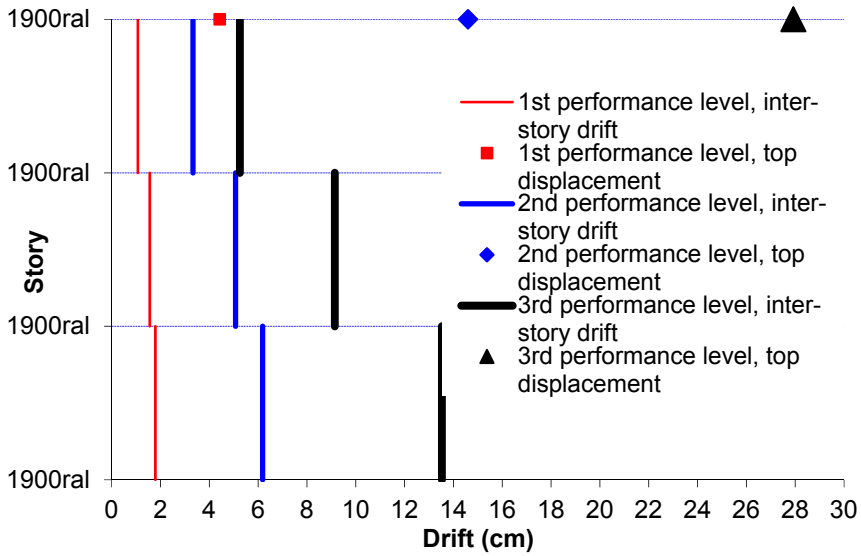

Figure 15: *Inter-story drifts and top displacement of 1st, 2nd and 3rd performance levels*

9.3 Discussions

It is generally accepted that the damage of structure is strain and displacement related. The residual top displacement can directly measure the global damage of structures subjected to the different earthquake hazard levels.

The estimate method of residual top displacement assumes that the steel frame is in hardening phase before it collapses. In this paper, the estimate method of residual top displacement only needs the displacement and base shear force at yield point. Therefore, the pushover analysis is used until steel frame yields (Inequalities Eq. (18) or Eq. (19) is true). The computational time to get the yield point is far less than that to use pushover analysis until the structure collapses. On the other hand, it is not easy to succeed in demonstrating pushover analysis until structures collapse because the different structures will be produced in the optimization process. However, it is easy to succeed in implementing pushover analysis until structures yield. Therefore, the optimization process will not be interrupted. The estimate method of residual top displacement can be used in optimization design of steel frames at serviceability, life safety, and collapse prevention levels. With the aid of Eq. (30) and Figure 9, it can be observed that the estimated value of residual top displacement is greater than the real residual top displacement. Therefore, the estimate method of residual top displacement is conservative. The residual top displacement can be calculated using the computational procedure discussed in Section 7.

The input peak ground accelerations, i.e., $a_g^{(1)}$ (serviceability), $a_g^{(2)}$ (life-safety), and $a_g^{(3)}$ (collapse prevention) are often given in the design codes. Therefore, it is only necessary to determine the limits on residual top displacements, i.e., $\left[D_{tp}^{(1)} \right]$, $\left[D_{tp}^{(2)} \right]$ and $\left[D_{tp}^{(3)} \right]$, in the optimization model Eq. (32). Then the optimization design of steel frames can be implemented. The example in this paper just shows how to implement a three-level performance-based optimization method of steel frames. Structural engineers should set up structural parameters and the limits on residual top displacements in real practice according to real structure and local design code, respectively.

The inverted triangular load pattern is in principle inaccurate for structures where higher mode effects are significant. It is accurate enough for structures where the first mode is dominant. Because of the fact that the non linear analysis (pushover analysis) is based on a time-independent displacement shape, it may not detect the structural weaknesses which may be generated when the structures' dynamics characteristics change after the formation of the first local plastic mechanism.

Many researches (Fajfar, 1999, 2000, 2002; Kreslin and Fajfar, 2012) indicate that the results obtained by using the N2 method are reasonably accurate provided that the structure oscillates predominantly in the first mode. Therefore, the N2 method has been implemented in Eurocode 8 (European Committee for Standardization, 2004). The estimate method of residual top displacement proposed in this paper is direct developed based on the N2 method. For most building structures, the first mode always dominates the vibration. The residual top displacement obtained by using the estimate method proposed in this paper is reasonably accurate for performance based design. The restriction of the proposed method in this paper is the same as the N2 method (Fajfar 2000).

10 CONCLUSIONS

In this paper, an estimate method of residual top displacement has been developed for steel frames subjected to three earthquake hazard levels. A three-level performance-based optimization model is proposed based on the estimate method of residual top displacement. The main conclusions are

(1) The estimate method of residual top displacement needs to use pushover analysis until steel frames yield. The residual top displacement is estimated by using the yield displacement value and yield loading value at the yield point. The estimated value of the residual top displacement obtained by the proposed method is greater than the real residual top displacement. The estimated value of residual top displacement is conservative.

(2) The computational time to get the yield point is far less than to get the collapse point. It is relatively easier to succeed in implementing pushover analysis until steel frame yields than until the frame collapses. It also doesn't need any engineering judgements to get the yield point and the optimization process will not be interrupted in the proposed method.

(3) A three-level performance-based optimization model is proposed in this paper. In the optimization model, the peak ground accelerations related to three earthquake hazard levels and the limits on residual top displacement related to the three performance levels are required to start optimization design. The peak ground accelerations are often given in design codes. However, the limits on residual top displacement related to life safety and collapse prevention levels should be further investigated in the future.

(4) The pushover analyses of the optimum design indicate that the steel frame is at elastic phase at serviceability level, at inelastic and hardening phases at life safety and collapse prevention levels. It means that the assumption of residual top displacement is reliable when it is used in three-level performance-based optimization model.

References

Applied Technology Council (1996) Seismic evaluation and retrofit of concrete buildings, Report ATC-40.

Aschheim M and Black EF (2000) Yield Point Spectra for Seismic Design and Rehabilitation. Earthquake Spectra16: 317-336.

European Committee for Standardization (2004) Eurocode 8: Design of structures for earthquake resistance - Part 1: general rules, seismic actions and rules for buildings. European standard EN 1998-1 (English Edition).

Fajfar P and Gaspersic P (1996) The N2 method for the seismic damage analysis of regular buildings. Earthquake Engineering and Structural Dynamics 25:23-67.

Fajfar P (1999) Capacity spectrum method based on inelastic demand spectrum. Earthquake Engineering and Structural Dynamics 28:979-993.

Fajfar P (2000) A nonlinear analysis method for performance based seismic design. Earthquake Spectra 16:573-592.

Fajfar P (2002) Structural analysis in earthquake engineering - a breakthrough of simplified non-linear methods. Paper Reference 843, Proceedings of 12th European Conference on Earthquake Engineering, London.

Freeman SA (1998) The capacity spectrum method as a tool for seismic design. Proceedings of the 11th European conference on earthquake engineering, Paris.

Gencturk B and Elnashai AS (2008) Development and application of an advanced capacity spectrum method. Engineering Structures 30:3345-3354.

Ghobarah A (2001) Performance-based design in earthquake engineering: state of development. Engineering Structures 23:878-884.

Ibrahimbegovic A (1995) On finite element implementation of geometrically nonlinear Reissner's beam theory: three-dimensional curved beam elements. Computer Method in Applied Mechanics and Engineering 26: 11-26.

Kreslin M and Fajfar P (2012) The extended N2 method considering higher mode effects in both plan and elevation. Bulletin of Earthquake Engineering 10:695-715.

Liu Q, Zhang J and Yan L (2010) An optimal method for seismic drift design of concrete buildings using gradient and Hessian matrix calculations. Archive of Applied Mechanics 80:1225-1242.

Liu Q and Paavola J (2015) An Optimization Procedure for Seismic Design of Steel Frames for Multi-Performance and Multi-Hazard Levels. Advances in Structural Engineering 18(1) 59-74.

Simo JC and Vu-Quoc L (1986) A three dimensional finite strain rod model. Part II: computational aspects. Computer Method in Applied Mechanics and Engineering 58: 79-116.

Vidic T, Fajfar P and Fischinger M (1994) Constant inelastic design spectra: strength and displacement, Earthquake Engineering and Structural Dynamics 23 (1994) 502-521.

Washington (DC): Federal Emergency Management Agency (2000) Prestandard and commentary for the seismic rehabilitation of buildings, Report FEMA-356.

Zou XK and Chan CM (2005) Optimal seismic performance-based design of reinforced concrete buildings using nonlinear pushover analysis. Engineering Structures 27:1289-1302.